Available online at www.sciencedirect.com
SCIENCE DIRECT®
Journal of Sound and Vibration 284 (2005) 851–878
JOURNAL OF SOUND AND VIBRATION
www.elsevier.com/locate/jsvi

Exact dynamic stiffness matrix of non-symmetric thin-walled curved beams subjected to initial axial force

Kim Nam-Il, Kim Moon-Young*

Department of Civil-Environmental Engineering, SungKyunKwan University, Jangan-Gu, Suwon, Kyoungki-Do, 440-746, South Korea

Received 2 January 2004; received in revised form 13 July 2004; accepted 19 July 2004

Available online 13 December 2004

Abstract

An improved numerical method to exactly evaluate the dynamic element stiffness matrix is proposed for the spatially coupled free vibration analysis of non-symmetric thin-walled curved beams subjected to uniform axial force. For this purpose, firstly equations of motion, boundary conditions and force–deformation relations are rigorously derived from the total potential energy for a curved beam element. Next systems of linear algebraic equations with non-symmetric matrices are constructed by introducing 14 displacement parameters and transforming the fourth-order simultaneous differential equations into the first-order simultaneous equations. And then explicit expressions for displacement parameters are numerically evaluated via eigensolutions and the exact 14×14 element stiffness matrix is determined using force–deformation relations. In order to demonstrate the validity and the accuracy of this study, the spatially coupled natural frequencies of non-symmetric thin-walled curved beams subjected to uniform compressive and tensile forces are evaluated and compared with analytical and finite element solutions using Hermitian curved beam elements or ABAQUS's shell element. In addition, some results by the parametric study are reported.

*Corresponding author. Tel.: +82 31 290 7514; fax: +82 31 290 7548.
E-mail address: kmye@skku.ac.kr (K. Moon-Young).

0022-460X/$ - see front matter © 2004 Elsevier Ltd. All rights reserved.
doi:10.1016/j.jsv.2004.07.006

1. Introduction

Thin-walled curved beam structures have been used in many civil, mechanical, and aerospace engineering applications such as curved wire, curved girder bridges, turbomachinery blade, tire dynamic, and stiffeners in aircraft structures. It can also be used as a simplified model of a shell structure. The vibrational behavior of non-symmetric thin-walled curved beam structures is very complex due to the coupling effect of extensional, bending, and torsional deformation. Due to this reason, it is not easy to evaluate exactly the natural frequencies of the spatially coupled thin-walled curved beam with non-symmetric cross-section.

Up to the present, the study for the free in-plane vibration [1–23] of curved beam have been done by considering various parameters such as boundary conditions, shear deformation, rotary inertia, variable curvatures and variable cross-sections. Particularly considerable research [1–8] was reported on the exact solutions for free in-plane vibration of curved beam. Nieh et al. [1] developed an analytical solution for the free vibration and stability of elliptic arches subjected to a uniformly distributed vertical static loading by incorporating series solutions and stiffness matrices. Eisenberger and Efraim [2] presented the exact dynamic stiffness matrix for a circular beam with a uniform cross-section. The matrix is derived from the differential equation of motion for a beam. This stiffness matrix is free of membrane and shear locking as the shape functions that are used are the exact solution of the differential equations of motion. Howson and Jemah [3] evaluated the planar natural frequency of curved Timoshenko beams with uniform cross-section and arbitrary boundary conditions. This is achieved by using exact dynamic stiffness matrix and by utilizing a new version of the Wittrick–Williams algorithm [24] which determines the number of natural frequencies exceeded by any trial frequency. Huang et al. [4] and Tseng et al. [5] provided the systematic approach to solve the in-plane vibrations of arches with variable cross-section and constant cross-section, respectively, using the Frobenius method [25] combined with the dynamic stiffness method. Gupta and Howson [6] presented a method for converging with certainty upon any required natural frequency of a plane slender curved beam. They used the exact member theory in conjunction with the dynamic stiffness technique and this necessitated the solution of a transcendental eigenvalue problem. Solutions were achieved by use of the Wittrick–Williams algorithm. Issa et al. [7] presented a unified theory which includes the effects of transverse shear and rotary inertia as well as the extensional effect of the neutral axis and derived the dynamic stiffness matrix for a circular curved beam in terms of rotational and translational displacements. Wang and Guilbert [8] derived the dynamic stiffness matrix formulation for circular curved beams of constant cross-section, including the effects of rotary inertia and shear deformation, for determination of the natural frequencies of continuous two-span curved beams.

On the other hand, the research for the free out-of-plane vibration of curved beam has been performed by several authors [26–36]. Lee and Chao [26] derived the governing differential equations for the out-of-plane vibrations of a curved non-uniform beam of constant radius via Hamilton's principle. With the explicit relations between the torsional displacement, its derivative and the flexural displacement, the two coupled governing characteristic differential equations are reduced to one sixth-order ordinary differential equation with variable coefficients in the out-of-plane flexural displacement. Huang et al. [27,28] developed the dynamic stiffness matrix for non-circular curved beams from a series of solution using the Frobenius method, with which an exact

solution of the out-of-plane free vibration of this type of beam was derived. Howson and Jemah [29] and Howson et al. [30] evaluated the required natural frequencies of out-of-plane motion of plane structures composed of Timoshenko and slender curved beams, respectively. The solution of the inherent transcendental eigenvalue problem was achieved through a variation on the Wittric–Williams algorithm. Kang et al. [31] computed the eigenvalues of free vibration of horizontally curved beams with doubly symmetric cross-section using the differential quadrature method (DQM).

Yildrim [37] numerically treated both in-plane and out-of-plane free vibrations of circular arch with doubly symmetrical cross-sections, considering the effects of shear and axial deformation and rotary inertia, with the help of the transfer matrix method. Kang et al. [38] applied the DQM to the computation of the eigenvalues of the equations of motion governing the free in-plane vibration including the extensibility of the arch axis with the effects of rotary inertia but neglecting shear deformation and the coupled out-of-plane twist-bending vibration of circular arches. Also they [39] obtained the fundamental frequency for the in-plane and out-of-plane vibration of rectangular and circular arches based on the Timoshenko beam theory using the DQM. Kawakami et al. [40] proposed an approximate method for analyzing the free in-plane and out-of-plane vibration of horizontally curved beams with arbitrary shapes and variable cross-sections. This method was based on a combination of numerical integration and numerical solution of integral equations.

Even though a significant amount of research has been conducted on development of exact solutions for in-plane and out-of-plane free vibration analysis of curved beam structures, to the author's knowledge, there was no study reported on the exact solutions for the spatially coupled free vibration of thin-walled curved beams with non-symmetric cross-section in the literature. Recently Kim et al. [41] presented an improved energy formulation for spatially coupled free vibration of thin-walled curved beams with non-symmetric cross-section neglecting shear deformation but considering rotary inertia and thickness-curvature effects. They derived only an analytical solutions for free in-plane and out-of-plane vibrations of curved beams with mono-symmetric cross-section which is symmetric for the plane of curvature. Furthermore, Kim et al. [42] proposed a new method evaluating the exact dynamic element stiffness matrix of thin-walled straight beams.

The primary aim of this study is to derive governing equations of harmonically vibrating non-symmetric thin-walled curved beams under initial axial force which constitute 4 simultaneous ordinary differential equations and to evaluate *the exact dynamic element stiffness matrix of those curved beams* based on the previous research [41,42]. For this purpose, equations of motion and force–deformation relations are first derived for a curved beam element. Next, the fourth-order simultaneous differential equations are transformed into a set of the first-order simultaneous ordinary differential equations by introducing 14 displacement parameters so that a generalized linear eigenvalue problem is obtained with non-symmetric matrices. And then using the solutions of the eigenproblem allowing the complex eigenvalues and eigenvectors, displacement functions of 14 displacement parameters are exactly derived with respect to nodal displacements. Finally, nodal forces are exactly evaluated using member force–deformation relationships and 14×14 dynamic element stiffness matrix of curved beams is determined.

In order to demonstrate the validity and the accuracy of this study, the spatially coupled natural frequencies are evaluated and compared with analytical solutions and the results by analysis using

the Hermitian curved beam elements [41] and ABAQUS's shell elements [43]. In addition, some results by the parametric study is reported.

2. Equations of motion for thin-walled curved beams

Fig. 1 shows the global coordinates of the non-symmetric thin-walled curved beam and Fig. 2(a) and (b) show displacement parameters and stress resultants of thin-walled curved beams, respectively. The x_1-axis coincides with the centroid axis and x_2, x_3-axis not necessarily principal axes. e_2, e_3 are components of the position vector of the shear center in the local coordinate. U_x, U_y, U_z and $\omega_1(=\theta), \omega_2, \omega_3$ are rigid-body translations and rotations with respect to x_1, x_2, x_3 axes, respectively, and f is a parameter defining warping. Stress resultants in Fig. 2(b) are defined by

$$F_1 = \int_A \tau_{11}\,\mathrm{d}A, \quad F_2 = \int_A \tau_{12}\,\mathrm{d}A, \quad F_3 = \int_A \tau_{13}\,\mathrm{d}A, \quad M_1 = \int_A (\tau_{13}x_2 - \tau_{12}x_3)\,\mathrm{d}A$$

$$M_2 = \int_A \tau_{11}x_3\,\mathrm{d}A, \quad M_3 = -\int_A \tau_{11}x_2\,\mathrm{d}A, \quad M_\phi = \int_A \tau_{11}\phi\,\mathrm{d}A, \tag{1}$$

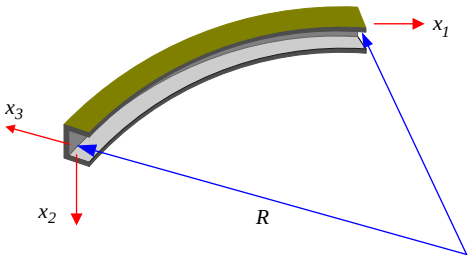

Fig. 1. A curvilinear coordinate system for non-symmetric thin-walled curved beams.

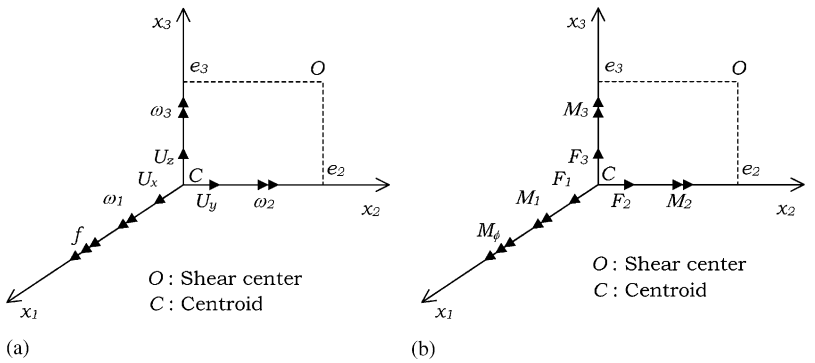

Fig. 2. Notation for displacement parameters and stress resultants. (a) Displacement parameters, (b) stress resultants.

where F_1, F_2 and F_3 = the axial, shear forces acting at the centroid, M_1, M_2 and M_3 = the total twist moment with respect to the centroid axis, bending moments with respect to x_2 and x_3 axes, respectively. M_R and M_ϕ = restrained torsional moment and the bimoment, respectively. It should be noticed that all stress resultants are defined with respect to the centroid.

The elastic strain energy including the effect of an initial axial force and the kinetic energy of thin-walled non-symmetric curved beam with the thickness-curvature effect and rotary inertia were derived in Ref. [41] and presented in Appendix A.

Now by variation of elastic strain and kinetic energies with respect to U_x, U_y, U_z and θ, equations of motion, boundary conditions and force–deformation relations for thin-walled curved beam are derived and expressed in Appendix B. It is evident that the equations of motion are a set of the fourth-order simultaneously ordinary differential equations because of coupling effects of bending-torsional deformations and non-symmetry of the cross-section.

3. Evaluation of dynamic stiffness matrix

In the next section, the exact dynamic stiffness matrix of a thin-walled curved beams with non-symmetric cross-section subjected to uniform compressive and tensile forces is derived.

3.1. Exact evaluation of displacement functions

In order to transform the equations of motion into a set of the first-order ordinary differential equations, a displacement state vector composed of 14 displacement parameters is defined by

$$\begin{aligned}\mathbf{d}(\mathbf{x}) &= \langle d_1, d_2, d_3, d_4, d_5, d_6, d_7, d_8, d_9, d_{10}, d_{11}, d_{12}, d_{13}, d_{14}\rangle^{\mathrm{T}} \\ &= \langle U_x, U_x', U_y, U_y', U_y'', U_y''', U_z, U_z', U_z'', U_z''', \theta, \theta', \theta'', \theta'''\rangle^{\mathrm{T}}.\end{aligned} \tag{2}$$

Now based on Eq. (2), the equations of motion are transformed into the following simultaneous ordinary differential equations of the first order with constant coefficients.

$$d_1' = d_2, \tag{3a}$$

$$\begin{aligned}-EAd_2' = {} & \left\{\rho\omega^2\left(A + \frac{2I_2}{R^2} + \frac{\tilde{I}_2}{R^2}\right) - \frac{1}{R^2}{}^0F_1\right\}d_1 - \rho\omega^2\frac{1}{R}\left\{\frac{1}{R}(\tilde{I}_{2\phi} + I_{2\phi}) + \left(\frac{I_{223}}{R} + 2I_{23}\right)\right\}d_4 \\ & + \left\{\frac{EA}{R} - \rho\omega^2\frac{1}{R}(\tilde{I}_2 + I_2) + \frac{1}{R}{}^0F_1\right\}d_8 - \rho\omega^2\frac{1}{R}(\tilde{I}_{2\phi} + I_{2\phi})d_{12},\end{aligned} \tag{3b}$$

$$d_3' = d_4, \tag{3c}$$

$$d_4' = d_5, \tag{3d}$$

$$d_5' = d_6, \tag{3e}$$

$$\left(E\hat{I}_3+\frac{1}{R^2}E\hat{I}_\phi+\frac{2}{R}E\hat{I}_{3\phi}\right)d'_6+\left(\frac{1}{R}E\hat{I}_{2\phi}+E\hat{I}_{23}\right)d'_{10}+\left(\frac{1}{R}E\hat{I}_\phi+E\hat{I}_{3\phi}\right)d'_{14}$$
$$=\rho\omega^2\frac{1}{R}\left(\frac{1}{R}\tilde{I}_{2\phi}+\frac{1}{R}I_{2\phi}+\frac{1}{R}I_{223}+2I_{23}\right)d_2+\rho\omega^2Ad_3+\left\{\frac{1}{R^2}GJ-\rho\omega^2\left(\tilde{I}_3+\frac{1}{R^2}\tilde{I}_\phi+\frac{2}{R}\tilde{I}_{3\phi}\right)\right.$$
$$\left.+{}^0F_1\left(1+\frac{\beta}{R^2}\right)\right\}d_5-\left\{\frac{1}{R^3}E\hat{I}_{2\phi}+\frac{1}{R^2}E\hat{I}_{23}+\rho\omega^2\left(\frac{1}{R}\tilde{I}_{2\phi}+\frac{1}{R}I_{223}+I_{23}\right)\right\}d_9-\frac{1}{R}\rho\omega^2I_2d_{11}$$
$$+\left\{\frac{1}{R}GJ+\frac{1}{R}E\hat{I}_3+\frac{1}{R^2}E\hat{I}_{3\phi}-\rho\omega^2\left(\frac{1}{R}\tilde{I}_\phi+\tilde{I}_{3\phi}\right)+\frac{\beta}{R}{}^0F_1\right\}d_{13}, \tag{3f}$$

$$d'_7=d_8, \tag{3g}$$

$$d'_8=d_9, \tag{3h}$$

$$d'_9=d_{10}, \tag{3i}$$

$$\left(\frac{1}{R}E\hat{I}_{2\phi}+E\hat{I}_{23}\right)d'_6+E\hat{I}_2d'_{10}+E\hat{I}_{2\phi}d'_{14}$$
$$=-\left\{\frac{1}{R}EA-\rho\omega^2\frac{1}{R}(\tilde{I}_2+I_2)+\frac{1}{R}{}^0F_1\right\}d_2$$
$$-\left\{\frac{1}{R^3}E\hat{I}_{2\phi}+\frac{1}{R^2}E\hat{I}_{23}+\rho\omega^2\left(\frac{1}{R}\tilde{I}_{2\phi}+\frac{1}{R}I_{223}+I_{23}\right)\right\}d_5-\left(\frac{1}{R^2}EA+\frac{1}{R^4}E\hat{I}_2-\rho\omega^2A\right)d_7$$
$$-\left(\frac{2}{R^2}E\hat{I}_2+\rho\omega^2\tilde{I}_2-{}^0F_1\right)d_9-\left(\frac{1}{R^3}E\hat{I}_{23}+\frac{1}{R}\rho\omega^2I_{23}\right)d_{11}$$
$$-\left(\frac{1}{R^2}E\hat{I}_{2\phi}-\frac{1}{R}E\hat{I}_{23}+\rho\omega^2\tilde{I}_{2\phi}\right)d_{13}, \tag{3j}$$

$$d'_{11}=d_{12}, \tag{3k}$$

$$d'_{12}=d_{13}, \tag{3l}$$

$$d'_{13}=d_{14}, \tag{3m}$$

$$\left(\frac{1}{R}E\hat{I}_\phi+E\hat{I}_{3\phi}\right)d'_6+E\hat{I}_{2\phi}d'_{10}+E\hat{I}_\phi d'_{14}$$
$$=\rho\omega^2\frac{1}{R}(\tilde{I}_{2\phi}+I_{2\phi})d_2-\rho\omega^2\frac{1}{R}I_2d_3+\left\{\frac{1}{R}GJ+\frac{1}{R}E\hat{I}_3\right.$$
$$\left.+\frac{1}{R^2}E\hat{I}_{3\phi}-\rho\omega^2\left(\frac{1}{R}\tilde{I}_\phi+\tilde{I}_{3\phi}\right)+\frac{\beta}{R}{}^0F_1\right\}d_5+\left(\frac{1}{R^3}E\hat{I}_{23}+\rho\omega^2\frac{1}{R}I_{23}\right)d_7$$

$$-\left(\frac{1}{R^2}E\hat{I}_{2\phi}-\frac{1}{R}E\hat{I}_{23}+\rho\omega^2\tilde{I}_{2\phi}\right)d_9-\left(\frac{1}{R^2}E\hat{I}_3-\rho\omega^2\tilde{I}_0-\frac{\beta}{R}{}^0F_1\right)d_{11}$$
$$+\left(GJ+\frac{2}{R}E\hat{I}_{3\phi}-\rho\omega^2\tilde{I}_\phi+\beta^0F_1\right)d_{13}, \tag{3n}$$

which can be compactly expressed as

$$\mathbf{A}\mathbf{d}'=\mathbf{B}\mathbf{d}, \tag{4}$$

where the detailed expressions for the matrices **A** and **B** are presented in Appendix C. In order to find the homogeneous solution of the simultaneous differential equation (4), the following eigenvalue problem with non-symmetric matrix is taken into account.

$$\lambda\mathbf{A}\mathbf{Z}=\mathbf{B}\mathbf{Z}. \tag{5}$$

In practice, the general eigenvalue problem (5) has the complex eigenvalue and the associated eigenvector because the matrix **A** is symmetric but **B** is non-symmetric. IMSL subroutine DGVCRG [44] is used in this study to obtain the complex eigensolutions of (5). From Eq. (5), 14 eigenvalues λ_i and 14×14 eigenvectors $\mathbf{Z}_i$ in complex domain can be calculated.

$$(\boldsymbol{\lambda}_i,\mathbf{Z}_i),\quad i=1,2,\ldots,14, \tag{6}$$

where

$$\mathbf{Z}_i=\langle z_{1i},z_{2i},z_{3i},z_{4i},z_{5i},z_{6i},z_{7i},z_{8i},z_{9i},z_{10i},z_{11i},z_{12i},z_{13i},z_{14i}\rangle^{\mathrm{T}}. \tag{7}$$

Based on the above eigensolutions, it is possible that the general solution of Eq. (4) is represented by the linear combination of eigenvectors with complex exponential functions as follows:

$$\mathbf{d}(\mathbf{x})=\sum_{i=1}^{14}\mathbf{a}_i\mathbf{Z}_i\mathrm{e}^{\lambda_i x}=\mathbf{X}(\mathbf{x})\mathbf{a}, \tag{8}$$

where

$$\mathbf{a}=\langle a_1,a_2,a_3,a_4,a_5,a_6,a_7,a_8,a_9,a_{10},a_{11},a_{12},a_{13},a_{14}\rangle^{\mathrm{T}} \tag{9a}$$

$$\mathbf{X}(\mathbf{x})=[\mathbf{Z}_1e^{\lambda_1x};\mathbf{Z}_2e^{\lambda_2x};\mathbf{Z}_3e^{\lambda_3x};\mathbf{Z}_4e^{\lambda_4x};\mathbf{Z}_5e^{\lambda_5x};\mathbf{Z}_6e^{\lambda_6x};\mathbf{Z}_7e^{\lambda_7x};$$
$$\mathbf{Z}_8e^{\lambda_8x};\mathbf{Z}_9e^{\lambda_9x};\mathbf{Z}_{10}e^{\lambda_{10}x};\mathbf{Z}_{11}e^{\lambda_{11}x};\mathbf{Z}_{12}e^{\lambda_{12}x};\mathbf{Z}_{13}e^{\lambda_{13}x};\mathbf{Z}_{14}e^{\lambda_{14}x}]. \tag{9b}$$

The **a** is the integration constant vector and **X**(**x**) denotes the 14×14 matrix function made up of 14 eigensolutions.

Now it is necessary that complex coefficient vector **a** is represented with respect to 14 nodal displacement components as shown in Fig. 3. For this, the following nodal displacement vector is defined by:

$$\mathbf{U}_e=\langle\mathbf{U}^p,\mathbf{U}^q\rangle^{\mathrm{T}}, \tag{10a}$$

$$\mathbf{U}^\alpha=\langle u^\alpha,v^\alpha,w^\alpha,\omega_1^\alpha,\omega_2^\alpha,\omega_3^\alpha,f^\alpha\rangle^{\mathrm{T}},\quad \alpha=p,q, \tag{10b}$$

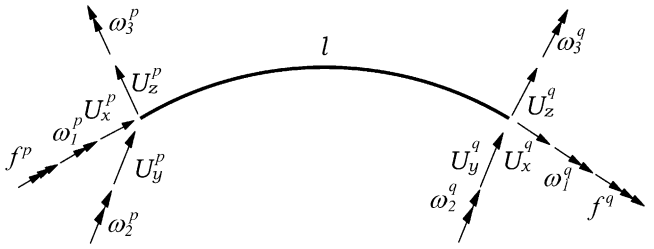

Fig. 3. Nodal displacement vector of a thin-walled curved beam element.

where

$$\mathbf{U}^p = \left\{ U_x(0), U_y(0), U_z(0), \theta(0), -\left(U_z' - \frac{1}{R}U_x\right)(0), U_y'(0), -\left(\theta' + \frac{1}{R}U_y'\right)(0) \right\}^{\mathrm{T}}, \tag{11a}$$

$$\mathbf{U}^q = \left\{ U_x(l), U_y(l), U_z(l), \theta(l), -\left(U_z' - \frac{1}{R}U_x\right)(l), U_y'(l), -\left(\theta' + \frac{1}{R}U_y'\right)(l) \right\}^{\mathrm{T}}. \tag{11b}$$

By substituting the coordinates of the member end ($x = 0, l$) into Eq. (8) and accounting for Eq. (11), the nodal displacement vector $\mathbf{U}_e$ is obtained as follows:

$$\mathbf{U}_e = \mathbf{E}\mathbf{a}, \tag{12}$$

where $\mathbf{E}$ is easily evaluated from $\mathbf{X}(\mathbf{x})$ and the detailed expression is

$$\mathbf{E} = \begin{bmatrix}
z_{1,1} & z_{1,2} & z_{1,3} & z_{1,4} & z_{1,5} & z_{1,6} & z_{1,7} & z_{1,8} & z_{1,9} & z_{1,10} & z_{1,11} & z_{1,12} & z_{1,13} & z_{1,14} \\
z_{3,1} & z_{3,2} & z_{3,3} & z_{3,4} & z_{3,5} & z_{3,6} & z_{3,7} & z_{3,8} & z_{3,9} & z_{3,10} & z_{3,11} & z_{3,12} & z_{3,13} & z_{3,14} \\
z_{7,1} & z_{7,2} & z_{7,3} & z_{7,4} & z_{7,5} & z_{7,6} & z_{7,7} & z_{7,8} & z_{7,9} & z_{7,10} & z_{7,11} & z_{7,12} & z_{7,13} & z_{7,14} \\
z_{11,1} & z_{11,2} & z_{11,3} & z_{11,4} & z_{11,5} & z_{11,6} & z_{11,7} & z_{11,8} & z_{11,9} & z_{11,10} & z_{11,11} & z_{11,12} & z_{11,13} & z_{11,14} \\
-z_{8,1} & -z_{8,2} & -z_{8,3} & -z_{8,4} & -z_{8,5} & -z_{8,6} & -z_{8,7} & -z_{8,8} & -z_{8,9} & -z_{8,10} & -z_{8,11} & -z_{8,12} & -z_{8,13} & -z_{8,14} \\
z_{4,1} & z_{4,2} & z_{4,3} & z_{4,4} & z_{4,5} & z_{4,6} & z_{4,7} & z_{4,8} & z_{4,9} & z_{4,10} & z_{4,11} & z_{4,12} & z_{4,13} & z_{4,14} \\
-z_{12,1} & -z_{12,2} & -z_{12,3} & -z_{12,4} & -z_{12,5} & -z_{12,6} & -z_{12,7} & -z_{12,8} & -z_{12,9} & -z_{12,10} & -z_{12,11} & -z_{12,12} & -z_{12,13} & -z_{12,14} \\
y_{1,1} & y_{1,2} & y_{1,3} & y_{1,4} & y_{1,5} & y_{1,6} & y_{1,7} & y_{1,8} & y_{1,9} & y_{1,10} & y_{1,11} & y_{1,12} & y_{1,13} & y_{1,14} \\
y_{3,1} & y_{3,2} & y_{3,3} & y_{3,4} & y_{3,5} & y_{3,6} & y_{3,7} & y_{3,8} & y_{3,9} & y_{3,10} & y_{3,11} & y_{3,12} & y_{3,13} & y_{3,14} \\
y_{7,1} & y_{7,2} & y_{7,3} & y_{7,4} & y_{7,5} & y_{7,6} & y_{7,7} & y_{7,8} & y_{7,9} & y_{7,10} & y_{7,11} & y_{7,12} & y_{7,13} & y_{7,14} \\
y_{11,1} & y_{11,2} & y_{11,3} & y_{11,4} & y_{11,5} & y_{11,6} & y_{11,7} & y_{11,8} & y_{11,9} & y_{11,10} & y_{11,11} & y_{11,12} & y_{11,13} & y_{11,14} \\
-y_{8,1} & -y_{8,2} & -y_{8,3} & -y_{8,4} & -y_{8,5} & -y_{8,6} & -y_{8,7} & -y_{8,8} & -y_{8,9} & -y_{8,10} & -y_{8,11} & -y_{8,12} & -y_{8,13} & -y_{8,14} \\
y_{4,1} & y_{4,2} & y_{4,3} & y_{4,4} & y_{4,5} & y_{4,6} & y_{4,7} & y_{4,8} & y_{4,9} & y_{4,10} & y_{4,11} & y_{4,12} & y_{4,13} & y_{4,14} \\
-y_{12,1} & -y_{12,2} & -y_{12,3} & -y_{12,4} & -y_{12,5} & -y_{12,6} & -y_{12,7} & -y_{12,8} & -y_{12,9} & -y_{12,10} & -y_{12,11} & -y_{12,12} & -y_{12,13} & -y_{12,14}
\end{bmatrix} \tag{13}$$

where $y_{ij} = z_{ij}e^{\lambda_j l}$, $i = 1, 3, 7, 11, 8, 4, 12$; $j =$ 1–14 and the inverse matrix of $\mathbf{E}$ is calculated using IMSL subroutine DLINCG [44].

Finally, elimination of the complex coefficient vector **a** from (12) and (8) yields the displacement state vector.

$$\mathbf{d}(\mathbf{x}) = \mathbf{X}(\mathbf{x})\mathbf{E}^{-1}\mathbf{U}_e \tag{14}$$

where $\mathbf{X}(\mathbf{x})\mathbf{E}^{-1}$ denotes the exact interpolation matrix.

3.2. Calculation of dynamic element stiffness matrix

Force–deformation relations of thin-walled curved beam can be rewritten with respect to 14 displacement parameters (2) as follows:

$$\begin{aligned} F_1 = {} & EAd_2 + \frac{1}{R}\left(E\hat{I}_{23} + \frac{1}{R}E\hat{I}_{2\phi}\right)d_5 + \frac{1}{R}\left(EA + \frac{1}{R^2}E\hat{I}_2\right)d_7 + \frac{1}{R}E\hat{I}_2 d_9 \\ & - \frac{1}{R^2}E\hat{I}_{23}d_{11} + \frac{1}{R}E\hat{I}_{2\phi}d_{13}, \end{aligned}$$

$$\begin{aligned} F_2 = {} & \rho\omega^2\frac{1}{R}\left(\frac{1}{R}\tilde{I}_{2\phi} + \frac{1}{R}I_{2\phi} + \frac{1}{R}I_{223} + 2I_{23}\right)d_1 \\ & + \left\{\frac{1}{R^2}GJ - \rho\omega^2\left(\tilde{I}_3 + \frac{1}{R^2}\tilde{I}_\phi + \frac{2}{R}\tilde{I}_{3\phi}\right) + {}^0F_1\left(1 + \frac{\beta}{R^2}\right)\right\}d_4 \\ & - \left(E\hat{I}_3 + \frac{1}{R^2}E\hat{I}_\phi + \frac{2}{R}E\hat{I}_{3\phi}\right)d_6 - \left\{\frac{1}{R^3}E\hat{I}_{2\phi} + \frac{1}{R^2}E\hat{I}_{23} + \rho\omega^2\left(\frac{1}{R}\tilde{I}_{2\phi} + \frac{1}{R}I_{223} + I_{23}\right)\right\}d_8 \\ & - \left(\frac{1}{R}E\hat{I}_{2\phi} + E\hat{I}_{23}\right)d_{10} + \left\{\frac{1}{R}GJ + \frac{1}{R}E\hat{I}_3 + \frac{1}{R^2}E\hat{I}_{3\phi}\right. \\ & \left. -\rho\omega^2\left(\frac{1}{R}\tilde{I}_\phi + \tilde{I}_{3\phi}\right) + \frac{\beta}{R}{}^0F_1\right\}d_{12} - \left(\frac{1}{R}E\hat{I}_\phi + E\hat{I}_{3\phi}\right)d_{14}, \end{aligned}$$

$$\begin{aligned} F_3 = {} & \frac{1}{R}\{\rho\omega^2(\tilde{I}_2 + I_2) - {}^0F_1\}d_1 - \rho\omega^2\left(\frac{1}{R}\tilde{I}_{2\phi} + \frac{1}{R}I_{223} + I_{23}\right)d_4 \\ & - \left(E\hat{I}_{23} + \frac{1}{R}E\hat{I}_{2\phi}\right)d_6 - \left(\frac{1}{R^2}E\hat{I}_2 + \rho\omega^2\tilde{I}_2 - {}^0F_1\right)d_8 - E\hat{I}_2 d_{10} \\ & + \left(\frac{1}{R}E\hat{I}_{23} - \rho\omega^2\tilde{I}_{2\phi}\right)d_{12} - E\hat{I}_{2\phi}d_{14}, \end{aligned}$$

$$\begin{aligned} M_1 = {} & \rho\omega^2\frac{1}{R}(\tilde{I}_{2\phi} + I_{2\phi})d_1 + \left\{\frac{1}{R}GJ - \rho\omega^2\left(\tilde{I}_{3\phi} + \frac{1}{R}\tilde{I}_\phi\right) + \frac{\beta}{R}{}^0F_1\right\}d_4 \\ & - \left(E\hat{I}_{3\phi} + \frac{1}{R}E\hat{I}_\phi\right)d_6 - \left(\frac{1}{R^2}E\hat{I}_{2\phi} + \rho\omega^2\tilde{I}_{2\phi}\right)d_8 - E\hat{I}_{2\phi}d_{10} \\ & + \left(GJ + \frac{1}{R}E\hat{I}_{3\phi} - \rho\omega^2\tilde{I}_\phi + \beta{}^0F_1\right)d_{12} - E\hat{I}_\phi d_{14}, \end{aligned}$$

$$M_2 = -\left(E\hat{I}_{23} + \frac{1}{R}E\hat{I}_{2\phi}\right)d_5 - \frac{1}{R^2}E\hat{I}_2 d_7 - E\hat{I}_2 d_9 + \frac{1}{R}E\hat{I}_{23}d_{11} - E\hat{I}_{2\phi}d_{13},$$

$$M_3 = \left(E\hat{I}_3 + \frac{1}{R}E\hat{I}_{3\phi}\right)d_5 + \frac{1}{R^2}E\hat{I}_{23}d_7 + E\hat{I}_{23}d_9 - \frac{1}{R}E\hat{I}_3 d_{11} + E\hat{I}_{3\phi}d_{13},$$

$$M_\phi = -\left(E\hat{I}_{3\phi} + \frac{1}{R}E\hat{I}_\phi\right)d_5 - \frac{1}{R^2}E\hat{I}_{2\phi}d_7 - E\hat{I}_{2\phi}d_9 + \frac{1}{R}E\hat{I}_{3\phi}d_{11} - E\hat{I}_\phi d_{13}, \tag{15a–g}$$

which is compactly represented as matrix form

$$\mathbf{f}(\mathbf{x}) = \mathbf{S}\mathbf{d}(\mathbf{x}), \tag{16}$$

where $\mathbf{f} = \langle F_1, F_2, F_3, M_1, M_2, M_3, M_\phi \rangle^{\mathrm{T}}$ and the components of 7×14 matrix $\mathbf{S}$ are expressed in Appendix D.

Now substituting Eq. (14) into Eq. (16) leads to

$$\mathbf{f}(\mathbf{x}) = \mathbf{S}\mathbf{X}(\mathbf{x})\mathbf{E}^{-1}\mathbf{U}_e. \tag{17}$$

Also the nodal force vector, as shown in Fig. 4 is defined by

$$\mathbf{F}_e = \langle \mathbf{F}^p, \mathbf{F}^q \rangle^{\mathrm{T}} \tag{18a}$$

$$\mathbf{F}^\alpha = \langle F_1^\alpha, F_2^\alpha, F_3^\alpha, M_1^\alpha, M_2^\alpha, M_3^\alpha, M_\phi^\alpha \rangle^{\mathrm{T}}, \quad \alpha = p, q. \tag{18b}$$

Therefore, nodal forces at ends of element ($x = 0, l$) are evaluated using Eq. (17) as

$$\mathbf{F}^p = -\mathbf{f}(\mathbf{o}) = -\mathbf{S}\mathbf{X}(\mathbf{o})\mathbf{E}^{-1}\mathbf{U}_e, \tag{19a}$$

$$\mathbf{F}^q = \mathbf{f}(\mathbf{l}) = \mathbf{S}\mathbf{X}(\mathbf{l})\mathbf{E}^{-1}\mathbf{U}_e. \tag{19b}$$

Consequently, the exact dynamic stiffness matrix $\mathbf{K}_d$ of a spatially coupled thin-walled curved beam element with non-symmetric cross-section is evaluated as follows:

$$\mathbf{F}_e = \mathbf{K}_d\mathbf{U}_e, \tag{20}$$

where

$$\mathbf{K}_d = \begin{bmatrix} -\mathbf{S}\mathbf{X}(0)\mathbf{E}^{-1} \\ \mathbf{S}\mathbf{X}(\mathbf{l})\mathbf{E}^{-1} \end{bmatrix}. \tag{21}$$

4. Numerical examples

In order to validate and conform the accuracy of the proposed method, the spatially coupled vibration analysis for the simply supported, fixed and cantilevered thin-walled curved beam with non-symmetric cross-sections are conducted and numerical results by the present study are compared with those by F. E. procedures [41], and ABAQUS's shell element.

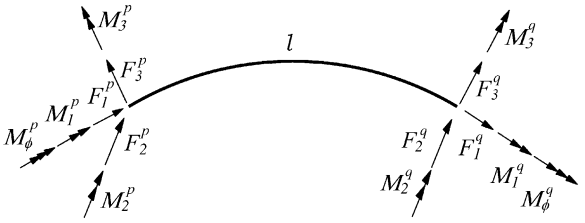

Fig. 4. Nodal force vector of a thin-walled curved beam element.

4.1. Simply supported curved beams with mono-symmetric cross-sections

We consider a simply supported curved beam having the cross-section mono-symmetric with respect to the x_3 axis. The geometric and material data are given in Fig. 5, in which the length of beams l are 100 and 400 cm, respectively. The subtended angles θ_0 for each length of beams are taken to be 30°and 90°, respectively. In this case, the in-plane and the out-of-plane vibration motions are decoupled. Table 1 shows the lowest five in-plane natural frequencies by this study with respect to the subtended angles for simply supported curved beams. For comparison, analytical solutions [41] and the results by 20 cubic Hermitian curved beam elements [41] are together presented. As can be seen in Table 1, the present solutions using only a single element coincide exactly with the analytical solutions and finite element solutions. It should be noted that the natural frequencies obtained from a single element based on the dynamic stiffness matrix gives exact results in the higher vibrational modes as well as the lower ones while a large number of beam elements in FE analysis are required to achieve the sufficient accuracy in the higher modes.

4.2. Simply supported, clamped and cantilevered beams with non-symmetric cross-sections

In this example, the spatially coupled free vibration analysis of simply supported, clamped and cantilevered curved beams with non-symmetric cross-section subjected to uniform axial force are performed. Fig. 6 shows the geometric and material data of curved beam with non-symmetric cross-section. This free vibration problem of curved beam with non-symmetric cross-section involves spatially coupled motions consisting of extension, flexure and twist. The subtended angle θ_0 of curved beam is taken to be 30°and the length of beam l is 200 cm. Here, the buckling loads of simply supported and clamped curved beams obtained from 20 Hermitian curved beam element are 22.29 and 141.58 N, respectively. The values of 11.145 and 70.79 N are adopted as initial forces for simply supported and clamped beams, respectively, which are the half of buckling loads of two curved beams. The lowest 10 spatially coupled natural frequencies of simply supported, clamped and cantilevered curved beams are presented in Tables 2–4, respectively. Also the present solutions are compared with the FE solutions obtained from various number of Hermitian curved beam elements. Particularly the results by 300 shell elements using the nine-noded shell elements(S9R5) of ABAQUS which is the commercial FE analysis program are together presented for a clamped and cantilevered curved beams without initial forces. From Tables 2–4, it can be

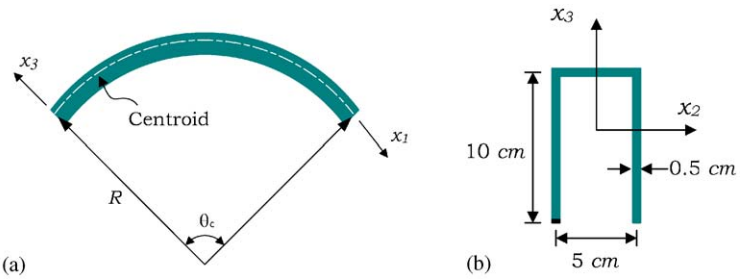

Fig. 5. Simply supported curved beam with mono-symmetric cross-section. (a) Simply supported curved beam. (b) Mono-symmetric cross-section. Material and section properties: $A = 12.5\,\mathrm{cm}^2$, $E = 73,000\,\mathrm{N/cm}^2$, $G = 28,000\,\mathrm{N/cm}^2$, $\rho = 0.00785\,\mathrm{N/cm}^3$, $J = 1.0417\,\mathrm{cm}^4$, $I_2 = 133.3854\,\mathrm{cm}^4$, $I_3 = 67.9167\,\mathrm{cm}^4$, $I_\phi = 5682.1302\,\mathrm{cm}^6$, $I_{\phi 3} = -585.1282\,\mathrm{cm}^5$, $I_{222} = -100\,\mathrm{cm}^5$, $I_{233} = -41.6667\,\mathrm{cm}^5$, $I_{\phi\phi 2} = 7465.7298\,\mathrm{cm}^7$, $I_{\phi 23} = -282.0513\,\mathrm{cm}^6$.

Table 1
In-plane natural frequencies of simply supported beam with mono-symmetric section, ω^2

l (cm)	θ_0 (deg)	Mode	This study	Analytic solution [41]	Finite element method [41]
		1	294.30	294.30	294.30
		2	1437.4	1437.4	1437.4
	30	3	7131.4	7131.4	7131.9
		4	9350.1	9350.1	9350.1
		5	21217	21217	21221
100					
		1	1105.1	1105.1	1105.1
		2	1800.3	1800.3	1800.4
	90	3	6890.8	6890.8	6891.3
		4	10586	10586	10586
		5	21038	21038	21043
		1	5.8260	5.8260	5.8261
		2	12.256	12.256	12.256
	30	3	32.501	32.501	32.503
		4	94.879	94.879	94.899
		5	232.02	232.02	232.14
400					
		1	4.4706	4.4706	4.4707
		2	24.049	24.049	24.050
	30	3	88.832	88.832	88.852
		4	126.16	126.16	126.17
		5	235.29	235.29	235.40

found that the present study yields exact solutions using only a single element, while at least 10 curved beam elements are demanded for the reasonably well results in the higher vibrational modes. As shown in Tables 3 and 4, the present solutions are in a good agreement with those of 'ABAQUS' shell element. Also it is noted from Tables 2 and 3 that the influence of initial

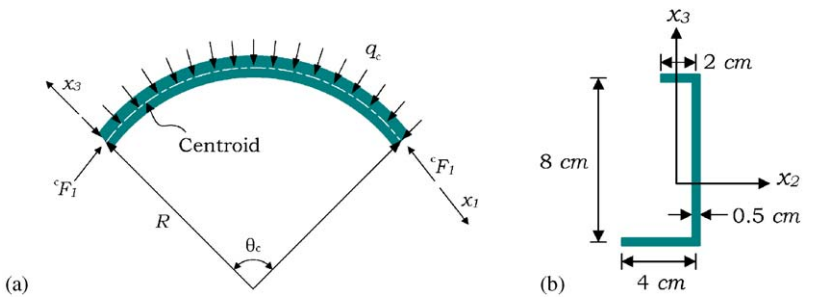

Fig. 6. Non-symmetric cross-section and material and section properties. (a) Under uniform compression load. (b) Cross-section. Material and section properties: $A = 7.0\,\text{cm}^2$, $E = 30,000\,\text{N/cm}^2$, $G = 11,500\,\text{N/cm}^2$, $J = 0.5833\,\text{cm}^4$, $\rho = 0.00785\,\text{N/cm}^3$, $I_2 = 67.0476\,\text{cm}^4$, $I_3 = 8.4286\,\text{cm}^4$, $I_{23} = 9.1429\,\text{cm}^4$, $I_{222} = 52.2449\,\text{cm}^5$, $I_{223} = -20.0272\,\text{cm}^5$, $I_{233} = -17.4150\,\text{cm}^5$, $I_{333} = -13.3878\,\text{cm}^5$, $I_\phi = 272.5442\,\text{cm}^6$, $I_{\phi 2} = 115.8095\,\text{cm}^5$, $I_{\phi 3} = 30.4762\,\text{cm}^5$, $I_{\phi 22} = 59.2109\,\text{cm}^6$, $I_{\phi 23} = -107.1020\,\text{cm}^6$, $I_{\phi 33} = -63.1293\,\text{cm}^6$, $I_{\phi\phi 2} = -67.1720\,\text{cm}^7$, $I_{\phi\phi 3} = -388.7269\,\text{cm}^7$.

compressive and tensile forces on the spatially coupled natural frequencies are predominant in the first few modes.

4.3. Some parametric study of curved beams with non-symmetric cross-section

In our final example, the effect of initial axial force on the spatially coupled natural frequency of curved beam with non-symmetric cross-section through the parametric study is investigated. First, we consider simply supported and clamped curved beams subjected to initial axial force. The same geometric and material data of curved beams as the one used in Section 4.2 are adopted (see Fig. 6) and the subtended angle is 90°and the length of beam is 100, 200, 300 and 400 cm. When the value of initial compressive and tensile force is 0.5 N, the lowest 10 spatially coupled natural frequencies of the simply supported and clamped curved beams by this study are presented in Tables 5 and 6, respectively.

Now the initial compressive forces are adopted as the value of the half of buckling load for two types of beams. Figs. 7 and 8 show the relative difference of the first two natural frequencies for simply supported and clamped beams subjected to initial compressive forces versus various subtended angle (see Fig. 7) and length of beam (see Fig. 8). In this example, the relative difference is defined by $(\omega_c^2 - \omega^2)/\omega^2 \times 100$, where ω_c denotes the frequency including the initial compressive force. It is interesting to observe from Figs. 7 and 8 that the effect of compressive forces on the fundamental frequency of simply supported beam is the same as the ratio 50% of these forces to buckling loads. However, those effects for clamped beams are a little smaller than those of simply supported beams and also, those effect on the second frequency of simply supported beams are less than those of clamped beams.

5. Conclusion

The higher-order simultaneous ordinary differential equations of non-symmetric thinwalled curved beams subjected to initial axial force are first derived and transformed into the first order

Table 2
Spatially coupled natural frequencies of simply supported beam with non-symmetric section, ω^2, ($\theta_0 = 30$, $P_{cr} = 22.290$ N)

l (cm)	Mode	This study	Finite element method				
			4	6	8	10	20
200	1	[0.049783]	[0.049889]	[0.049804]	[0.049790]	[0.049786]	[0.049783]
		0.099583	0.099689	0.099604	0.099590	0.099586	0.099583
		(0.14938)	(0.14949)	(0.14940)	(0.14939)	(0.14939)	(0.14938)
	2	[1.9801]	[1.9999]	[1.9842]	[1.9815]	[1.9807]	[1.9802]
		2.1784	2.1982	2.1825	2.1797	2.1789	2.1784
		(2.3766)	(2.3965)	(2.3807)	(2.3779)	(2.3772)	(2.3767)
	3	[8.4053]	[8.4079]	[8.4060]	[8.4056]	[8.4055]	[8.4054]
		8.4571	8.4593	8.4577	8.4574	8.4573	8.4573
		(8.5085)	(8.5104)	(8.5090)	(8.5087)	(8.5087)	(8.5086)
	4	[10.197]	[10.554]	[10.274]	[10.222]	[10.207]	[10.198]
		10.638	10.997	10.715	10.663	10.648	10.639
		(11.079)	(11.440)	(11.157)	(11.105)	(11.090)	(11.080)
	5	[13.138]	[13.197]	[13.150]	[13.141]	[13.139]	[13.138]
		13.335	13.394	13.347	13.339	13.336	13.335
		(13.532)	(13.591)	(13.544)	(13.536)	(13.534)	(13.532)
	6	[22.544]	[22.620]	[22.562]	[22.550]	[22.546]	[22.544]
		22.610	22.684	22.627	22.616	22.612	22.610
		(22.675)	(22.748)	(22.693)	(22.681)	(22.678)	(22.676)
	7	[29.730]	[35.424]	[30.331]	[29.930]	[29.814]	[29.736]
		30.518	36.222	31.121	30.718	30.602	30.524
		(31.306)	(37.020)	(31.910)	(31.506)	(31.390)	(31.312)
	8	[45.068]	[45.954]	[45.259]	[45.130]	[45.094]	[45.070]
		45.505	46.395	45.697	45.568	45.532	45.508
		(45.944)	(46.835)	(46.136)	(46.006)	(45.970)	(45.946)
	9	[58.199]	[58.546]	[58.270]	[58.222]	[58.209]	[58.200]
		58.394	58.742	58.465	58.417	58.404	58.395
		(58.590)	(58.937)	(58.660)	(58.612)	(58.599)	(58.590)
	10	[66.441]	[81.160]	[69.372]	[67.454]	[66.871]	[66.470]
		67.670	82.415	70.607	68.684	68.100	67.699
		(68.899)	(83.671)	(71.842)	(69.914)	(69.329)	(68.928)

Note: [ ] natural frequency with an initial compressive force 11.145 N.
( ) natural frequency with an initial tensile force 11.145 N.

Table 3
Spatially coupled natural frequencies of clamped beam with non-symmetric section, ω^2 ($\theta_0 = 30^\circ$, $P_{cr} = 141.58$ N)

l (cm)	Mode	This study	Finite element method					ABAQUS
			4	6	8	10	20	[43]
200	1	[0.42724]	[0.43232]	[0.42836]	[0.42761]	[0.42740]	[0.42725]	—
		0.83382	0.83643	0.83437	0.83400	0.83390	0.83383	0.8479
		(1.2271)	(1.2300)	(1.2277)	(1.2273)	(1.2272)	(1.2271)	—
	2	[3.9076]	[4.0010]	[3.9292]	[3.9148]	[3.9106]	[3.9078]	—
		5.3734	5.4752	5.3961	5.3810	5.3766	5.3737	5.4097
		(6.8218)	(6.9425)	(6.8487)	(6.8310)	(6.8258)	(6.8222)	—
	3	[10.380]	[10.440]	[10.397]	[10.386]	[10.383]	[10.380]	—
		10.770	10.834	10.788	10.777	10.773	10.770	10.605
		(11.150)	(11.220)	(11.171)	(11.158)	(11.154)	(11.150)	—
	4	[15.090]	[15.735]	[15.313]	[15.165]	[15.122]	[15.093]	—
		18.119	18.917	18.360	18.200	18.153	18.122	18.235
		(21.115)	(20.069)	(21.381)	(21.204)	(21.153)	(21.117)	—
	5	[20.638]	[21.118]	[20.749]	[20.677]	[20.655]	[20.640]	—
		22.086	22.591	22.205	22.128	22.104	22.087	21.878
		(23.526)	(24.062)	(23.656)	(23.573)	(23.547)	(23.528)	—
	6	[30.714]	[31.049]	[30.819]	[30.751]	[30.730]	[30.715]	—
		31.304	31.600	31.398	31.337	31.319	31.305	30.386
		(31.909)	(32.174)	(31.993)	(31.939)	(31.922)	(31.910)	—
	7	[39.806]	[52.901]	[41.124]	[40.273]	[40.004]	[39.820]	—
		45.192	58.798	46.592	45.680	45.398	45.206	45.524
		(50.573)	(64.697)	(52.067)	(51.088)	(50.789)	(50.588)	—
	8	[65.242]	[68.008]	[66.085]	[65.524]	[65.361]	[65.250]	—
		68.345	71.255	69.207	68.633	68.467	68.354	67.401
		(71.449)	(74.513)	(72.335)	(71.745)	(71.574)	(71.458)	—
	9	[84.744]	[125.19]	[88.275]	[86.739]	[85.608]	[84.802]	—
		93.019	126.64	96.891	95.086	93.908	93.078	93.276
		(101.30)	(128.10)	(105.52)	(103.45)	(102.22)	(101.36)	—
	10	[122.34]	[135.01]	[123.13]	[122.61]	[122.46]	[122.35]	—
		123.90	144.69	124.61	124.14	124.00	123.90	107.62
		(125.42)	(154.37)	(126.09)	(125.64)	(125.51)	(125.42)	—

Note: [ ] natural frequency with an initial compressive force 70.79 N.
( ) natural frequency with an initial tensile force 70.79 N.

Table 4
Spatially coupled natural frequencies of cantilevered beam with non-symmetric section, ω^2 ($\theta_0 = 30^\circ$)

l (cm)	Mode	This study	Finite element method					ABAQUS
			4	6	8	10	20	[43]
	1	0.0212	0.0214	0.0213	0.0212	0.0212	0.0212	0.0213
	2	0.2815	0.2819	0.2816	0.2816	0.2815	0.2815	0.2791
	3	0.3747	0.3753	0.3748	0.3747	0.3747	0.3747	0.3724
	4	2.2663	2.2772	2.2689	2.2673	2.2669	2.2666	2.2487
	5	5.0552	5.1030	5.0674	5.0596	5.0572	5.0554	5.0275
200								
	6	7.4325	7.5507	7.4598	7.4417	7.4364	7.4328	7.3378
	7	19.490	20.021	19.714	19.569	19.524	19.493	19.518
	8	20.510	20.742	20.564	20.530	20.519	20.511	19.935
	9	28.177	28.771	28.362	28.239	28.202	28.177	27.449
	10	49.050	60.347	50.466	49.585	49.283	49.067	49.227

Table 5
Spatially coupled natural frequencies of simply supported beam with various length, ω^2 ($\theta_0 = 90^\circ$)

Mode	Length of beam, l (cm)			
	100 $P_{cr} = 14.587\,\mathrm{N}$	200 $P_{cr} = 3.1907\,\mathrm{N}$	300 $P_{cr} = 1.4010\,\mathrm{N}$	400 $P_{cr} = 0.79124\,\mathrm{N}$
1	[0.24561] 0.25432 (0.26304)	[0.011983] 0.014210 (0.016437)	[0.0017912] 0.0027853 (0.0037794)	[0.00032623] 0.00088631 (0.0014464)
2	[11.363] 11.396 (11.429)	[0.83036] 0.83912 (0.84788)	[0.17593] 0.17987 (0.18382)	[0.057379] 0.059609 (0.061839)
3	[74.226] 74.299 (74.372)	[5.9088] 5.9283 (5.9477)	[1.3375] 1.3463 (1.3551)	[0.45718] 0.46217 (0.46717)
4	[168.05] 168.08 (168.11)	[15.231] 15.238 (15.246)	[3.5368] 3.5398 (3.5429)	[1.2114] 1.2131 (1.2148)
5	[188.19] 188.20 (188.21)	[20.523] 20.557 (20.592)	[4.8301] 4.8457 (4.8612)	[1.7051] 1.7140 (1.7228)
6	[252.88] 253.01 (253.14)	[36.718] 36.721 (36.723)	[12.156] 12.181 (12.205)	[4.3993] 4.4131 (4.4269)

Table 5 (*continued*)

Mode	Length of beam, l (cm)			
	100 $P_{cr} = 14.587\,\mathrm{N}$	200 $P_{cr} = 3.1907\,\mathrm{N}$	300 $P_{cr} = 1.4010\,\mathrm{N}$	400 $P_{cr} = 0.79124\,\mathrm{N}$
7	[557.52] 557.58 (557.64)	[50.578] 50.630 (50.682)	[14.236] 14.243 (14.251)	[5.3894] 5.3936 (5.3978)
8	[633.89] 634.08 (634.27)	[55.064] 55.083 (55.102)	[15.152] 15.153 (15.155)	[8.1551] 8.1556 (8.1562)
9	[858.33] 858.37 (858.40)	[90.364] 90.373 (90.382)	[25.002] 25.037 (25.072)	[9.1775] 9.1973 (9.2171)
10	[892.94] 892.98 (893.03)	[104.10] 104.18 (104.25)	[29.000] 29.004 (29.008)	[13.924] 13.927 (13.929)

Note: [ ] natural frequency with an initial compressive force 0.5 N.
( ) natural frequency with an initial tensile force 0.5 N.

Table 6
Spatially coupled natural frequencies of clamped beam with various length, ω^2 ($\theta_0 = 90^\circ$)

Mode	Length of beam, l (cm)			
	100 $P_{cr} = 395.26\,\mathrm{N}$	200 $P_{cr} = 103.04\,\mathrm{N}$	300 $P_{cr} = 46.733\,\mathrm{N}$	400 $P_{cr} = 26.611\,\mathrm{N}$
1	[10.525] 10.538 (10.550)	[0.71894] 0.72218 (0.72542)	[0.14310] 0.14455 (0.14600)	[0.044931] 0.045745 (0.046557)
2	[47.167] 47.207 (47.247)	[3.9805] 3.9913 (4.0020)	[0.87998] 0.88486 (0.88974)	[0.29309] 0.29585 (0.29861)
3	[157.20] 157.28 (157.36)	[13.546] 13.567 (13.589)	[3.2201] 3.2299 (3.2398)	[1.1291] 1.1347 (1.1403)
4	[247.40] 247.41 (247.42)	[31.817] 31.826 (31.835)	[8.2442] 8.2514 (8.2585)	[2.9626] 2.9685 (2.9743)
5	[326.71] 326.77 (326.79)	[35.173] 35.210 (35.247)	[8.5854] 8.5987 (8.6122)	[3.1760] 3.1818 (3.1876)

Table 6 (*continued*)

Mode	Length of beam, l (cm)			
	100 $P_{cr} = 395.26$ N	200 $P_{cr} = 103.04$ N	300 $P_{cr} = 46.733$ N	400 $P_{cr} = 26.611$ N
6	[426.49] 426.63 (426.77)	[41.841] 41.844 (41.846)	[16.057] 16.060 (16.063)	[6.6426] 6.6566 (6.6706)
7	[700.04] 700.08 (700.12)	[70.917] 70.955 (70.992)	[18.098] 18.120 (18.141)	[7.9268] 7.9314 (7.9360)
8	[960.12] 960.32 (960.53)	[80.545] 80.583 (80.620)	[20.554] 20.564 (20.575)	[8.6875] 8.6887 (8.6899)
9	[1200.0] 1200.0 (1200.1)	[138.02] 138.07 (138.12)	[33.580] 33.613 (33.645)	[12.550] 12.570 (12.590)
10	[1724.7] 1724.7 (1724.7)	[148.74] 148.78 (148.82)	[38.897] 38.906 (38.915)	[16.476] 16.480 (16.484)

Note: [ ] natural frequency with an initial compressive force 0.5 N.
( ) natural frequency with an initial tensile force 0.5 N.

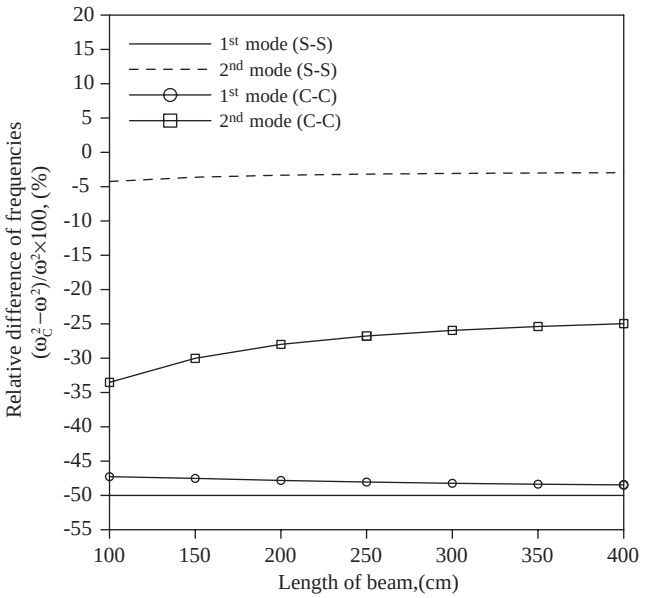

Fig. 7. Relative difference of natural frequencies versus length of beam due to an initial compressive force ($\theta_0 = 90^\circ$).

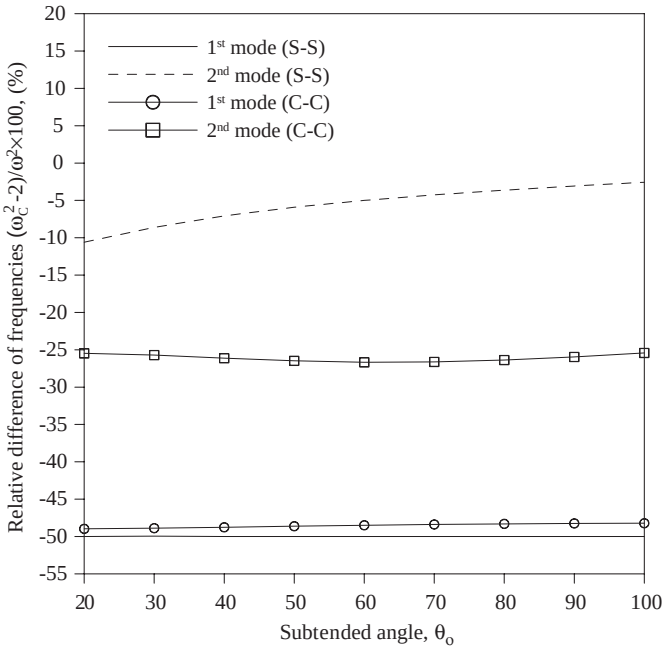

Fig. 8. Relative difference of natural frequencies versus subtended angle due to an initial compressive force ($l = 300$ cm).

differential equations. And then exact solutions of displacement parameters are obtained using a generalized linear eigenproblem having complex eigenvalues. Finally, dynamic element stiffness matrix of the harmonically vibrating curved beams subjected to axial force is determined using member force–displacement relationships. For spatially coupled natural frequencies of thin-walled curved beams under initial axial force, it is demonstrated that numerical results by the present method are in a good agreement with those by thin-walled beam elements and ABAQUS's shell element.

Consequently it is believed that the present procedure is general enough to provide a systematic tool for exact solutions of simultaneous ordinary differential equations of the higher order with constant coefficients.

Acknowledgements

This work is a part of a research project supported by a Grant (R01-2002-000-00265-0) from the Korea Science and Engineering Foundation and Korea Ministry of Construction & Transportation through Korea Bridge Design & Engineering Research Center at Seoul National University and the authors wish to express their gratitude for the financial support.

Appendix A

A.1. The elastic strain energy including the effect of an initial axial force

$$\begin{aligned}\Pi_E = \frac{1}{2}\int_0^L \Bigg[& EA\left(U_x' + \frac{U_z}{R}\right)^2 + E\hat{I}_2\left(U_z'' + \frac{U_z}{R^2}\right)^2 + E\hat{I}_3\left(U_y'' - \frac{\theta}{R}\right)^2 + E\hat{I}_\phi\left(\theta'' + \frac{U_y''}{R}\right)^2 \\ & + GJ\left(\theta' + \frac{U_y'}{R}\right)^2 + 2E\hat{I}_{2\phi}\left(U_z'' + \frac{U_z}{R^2}\right)\left(\theta'' + \frac{U_y''}{R}\right) + 2E\hat{I}_{3\phi}\left(U_y'' - \frac{\theta}{R}\right)\left(\theta'' + \frac{U_y''}{R}\right) \\ & + 2E\hat{I}_{23}\left(U_y'' - \frac{\theta}{R}\right)\left(U_z'' + \frac{U_z}{R^2}\right) + {}^0F_1\left\{U_y'^2 + \left(U_z' - \frac{U_x}{R}\right)^2\right\} \\ & + {}^0F_1\beta\left(\omega_1' + \frac{\omega_3}{R}\right)^2\Bigg]\mathrm{d}x_1, \end{aligned} \tag{A.1}$$

where

$$\begin{gathered}\hat{I}_2 = I_2 - \frac{I_{222}}{R}, \quad \hat{I}_3 = I_3 - \frac{I_{233}}{R}, \quad \hat{I}_\phi = I_\phi - \frac{I_{\phi\phi 2}}{R}, \\ \hat{I}_{\phi 2} = I_{\phi 2} - \frac{I_{\phi 22}}{R}, \quad \hat{I}_{\phi 3} = I_{\phi 3} - \frac{I_{\phi 23}}{R}, \quad \hat{I}_{23} = I_{23} - \frac{I_{223}}{R}, \quad \beta = \frac{I_2 + I_3}{A}. \end{gathered} \tag{A.2}$$

A.2. The kinetic energy

$$\begin{aligned}\Pi_M = \frac{1}{2}\rho\omega^2\int_0^L \Bigg\{ & A(U_x^2 + U_y^2 + U_z^2) + \tilde{I}_0\theta^2 + \tilde{I}_2\left(U_z' - \frac{U_x}{R}\right)^2 \\ & - 2\frac{I_2}{R}U_y\theta - 2\frac{I_2}{R}U_x\left(U_z' - \frac{U_x}{R}\right) + \tilde{I}_3U_y'^2 + \tilde{I}_\phi\left(\theta' + \frac{U_y'}{R}\right)^2 \\ & + 2\tilde{I}_{3\phi}U_y'\left(\theta' + \frac{U_y'}{R}\right) + 2\tilde{I}_{2\phi}\left(U_z' - \frac{U_x}{R}\right)\left(\theta' + \frac{U_y'}{R}\right) \\ & - 2\frac{I_{2\phi}}{R}U_x\left(\theta' + \frac{U_y'}{R}\right) + 2\frac{I_{223}}{R}U_y'\left(U_z' - \frac{U_x}{R}\right) \\ & + 2I_{23}\left(U_y'U_z' - \frac{2}{R}U_xU_y' + \frac{1}{R}U_z\theta\right)\Bigg\}\mathrm{d}x_1, \end{aligned} \tag{A.3}$$

where

$$\begin{gathered}\tilde{I}_2 = I_2 + \frac{I_{222}}{R}, \quad \tilde{I}_3 = I_3 + \frac{I_{233}}{R}, \quad \tilde{I}_\phi = I_\phi + \frac{I_{\phi\phi 2}}{R}, \quad I_0 = I_2 + I_3, \\ \tilde{I}_{\phi 2} = I_{\phi 2} + \frac{I_{\phi 22}}{R}, \quad \tilde{I}_{\phi 3} = I_{\phi 3} + \frac{I_{\phi 23}}{R}, \quad \tilde{I}_0 = I_0 + \frac{I_{222} + I_{233}}{R}, \end{gathered} \tag{A.4}$$

in which E and G = the Young's modulus and shear modulus, J and ρ = torsional constant and density. $I_2, I_3, I_{23}, I_{222}, I_{223}, I_{233}, I_\phi, I_{2\phi}, I_{3\phi}, I_{\phi 22}, I_{\phi 23}, I_{\phi\phi 2}$ = sectional constants of which the detailed expressions may be referred to Ref. [41]. The superscript 'prime' denotes the derivative with respect to x_1.

Appendix B

B.1. Equations of motion of thin-walled curved beams

$$
\begin{aligned}
&-EA\left(U_x''+\frac{1}{R}U_z'\right)-\rho\omega^2\left(A+\frac{1}{R^2}I_2\right)U_x+\rho\omega^2\frac{1}{R}(\tilde{I}_2+I_2)\left(U_z'-\frac{1}{R}U_x\right)\\
&+\rho\omega^2\frac{1}{R}(\tilde{I}_{2\phi}+I_{2\phi})\left(\theta'+\frac{1}{R}U_y'\right)+\rho\omega^2\frac{1}{R}\left(\frac{1}{R}I_{223}+2I_{23}\right)U_y'-\frac{1}{R}{}^0F_1\left(U_z'-\frac{U_x}{R}\right)=0,
\end{aligned}
\tag{B.1a}
$$

$$
\begin{aligned}
&E\hat{I}_3\left(U_y''''-\frac{1}{R}\theta''\right)+\frac{1}{R}E\hat{I}_\phi\left(\theta''''+\frac{1}{R}U_y''''\right)-\frac{1}{R}GJ\left(\theta''+\frac{1}{R}U_y''\right)\\
&\quad+\frac{1}{R}E\hat{I}_{2\phi}\left(U_z''''+\frac{1}{R^2}U_z''\right)+E\hat{I}_{3\phi}\left\{\frac{1}{R}\left(U_y''''-\frac{1}{R}\theta''\right)+\left(\theta''''+\frac{1}{R}U_y''''\right)\right\}\\
&\quad+E\hat{I}_{23}\left(U_z''''+\frac{1}{R^2}U_z''\right)-\rho\omega^2AU_y+\rho\omega^2\frac{1}{R}\left(I_2+\tilde{I}_3+\frac{1}{R}\tilde{I}_{3\phi}\right)\theta\\
&\quad+\rho\omega^2\left(\tilde{I}_3+\frac{1}{R}\tilde{I}_{3\phi}\right)\left(U_y''-\frac{1}{R}\theta\right)+\rho\omega^2\left(\frac{1}{R}\tilde{I}_\phi+\tilde{I}_{3\phi}\right)\left(\theta''+\frac{1}{R}U_y''\right)\\
&\quad+\rho\omega^2\left(\frac{1}{R}\tilde{I}_{2\phi}+\frac{1}{R}I_{223}+I_{23}\right)\left(U_z''+\frac{1}{R^2}U_z\right)+\rho\omega^2\frac{1}{R^2}\left(\frac{1}{R}I_{2\phi}+I_{23}\right)U_z\\
&\quad-\rho\omega^2\frac{1}{R}\left(\frac{1}{R}\tilde{I}_{2\phi}+\frac{1}{R}I_{2\phi}+\frac{1}{R}I_{223}+2I_{23}\right)\left(U_x+\frac{1}{R}U_z\right)\\
&\quad-{}^0F_1\left(1+\frac{\beta}{R^2}\right)U_y''-{}^0F_1\frac{\beta}{R}\theta''=0,
\end{aligned}
\tag{B.1b}
$$

$$
\begin{aligned}
&\frac{1}{R}EA\left(U_x'+\frac{1}{R}U_z\right)+E\hat{I}_2\left\{\left(U_z''''+\frac{1}{R^2}U_z''\right)+\frac{1}{R^2}\left(U_z''+\frac{1}{R^2}U_z\right)\right\}\\
&\quad+E\hat{I}_{2\phi}\left\{\left(\theta''''+\frac{1}{R}U_y''''\right)+\frac{1}{R^2}\left(\theta''+\frac{1}{R}U_y''\right)\right\}+E\hat{I}_{23}\left\{\left(U_y''''-\frac{1}{R}\theta''\right)\right.\\
&\quad\left.+\frac{1}{R^2}\left(U_y''-\frac{1}{R}\theta\right)\right\}-\rho\omega^2\left(A-\frac{1}{R^2}I_2\right)U_z+\rho\omega^2\tilde{I}_2\left(U_z''+\frac{1}{R^2}U_z\right)
\end{aligned}
$$

$$
\begin{aligned}
&- \rho\omega^2 \frac{1}{R}(\tilde{I}_2 + I_2)\left(U'_x + \frac{1}{R}U_z\right) + \rho\omega^2 \tilde{I}_{2\phi}\left(\theta'' + \frac{1}{R}U''_y\right) \\
&+ \rho\omega^2\left(\frac{1}{R}I_{223} + I_{23}\right)\left(U''_y - \frac{1}{R}\theta\right) + \rho\omega^2 \frac{1}{R^2}I_{223}\theta - {}^0F_1\left(U''_z - \frac{U'_x}{R}\right) = 0,
\end{aligned} \tag{B.1c}
$$

$$
\begin{aligned}
&- \frac{1}{R}E\hat{I}_3\left(U''_y - \frac{1}{R}\theta\right) + E\hat{I}_\phi\left(\theta'''' + \frac{1}{R}U''''_y\right) - GJ\left(\theta'' + \frac{1}{R}U''_y\right) + E\hat{I}_{2\phi}\left(U''''_z + \frac{1}{R^2}U''_z\right) \\
&+ E\hat{I}_{3\phi}\left\{\left(U''''_y - \frac{1}{R}\theta''\right) - \frac{1}{R}\left(\theta'' + \frac{1}{R}U''_y\right)\right\} - \frac{1}{R}E\hat{I}_{23}\left(U''_z + \frac{1}{R^2}U_z\right) - \rho\omega^2\left(\tilde{I}_0 - \frac{1}{R}\tilde{I}_{3\phi}\right)\theta \\
&+ \rho\omega^2 \frac{1}{R}I_2 U_y + \rho\omega^2 \tilde{I}_\phi\left(\theta'' + \frac{1}{R}U''_y\right) + \rho\omega^2 \tilde{I}_{3\phi}\left(U''_y - \frac{1}{R}\theta\right) + \rho\omega^2 \tilde{I}_{2\phi}\left(U''_z + \frac{1}{R^2}U_z\right) \\
&- \rho\omega^2 \frac{1}{R}(\tilde{I}_{2\phi} + I_{2\phi})\left(U'_x + \frac{1}{R}U_z\right) + \rho\omega^2 \frac{1}{R}\left(\frac{1}{R}I_{2\phi} - I_{23}\right)U_z - {}^0F_1\beta\left(\theta'' + \frac{U''_y}{R}\right) = 0.
\end{aligned} \tag{B.1d}
$$

B.2. Boundary conditions of thin-walled curved beams

$$\delta U_x(o) = \delta U_x^p; \quad \delta U_x(l) = \delta U_x^q, \tag{B.2a,b}$$

$$\delta U_y(o) = \delta U_y^p; \quad \delta U_y(l) = \delta U_y^q, \tag{B.2c,d}$$

$$\delta U_z(o) = \delta U_z^p; \quad \delta U_z(l) = \delta U_z^q, \tag{B.2e,f}$$

$$\delta\theta(o) = \delta\omega_1^p; \quad \delta\theta(l) = \delta\omega_1^q, \tag{B.2g,h}$$

$$-\delta\left(U'_z - \frac{1}{R}U_x\right)(0) = \delta\omega_2^p; \quad -\delta\left(U'_z - \frac{1}{R}U_x\right)(l) = \delta\omega_2^q, \tag{B.2i,j}$$

$$\delta U'_y(o) = \delta\omega_3^p; \quad \delta U'_y(l) = \delta\omega_3^q, \tag{B.2k,l}$$

$$-\delta\left(\theta' + \frac{1}{R}U'_y\right)(0) = \delta f^p; \quad -\delta\left(\theta' + \frac{1}{R}U'_y\right)(l) = \delta f^q. \tag{B.2m,n}$$

B.3. Force–deformation relations

$$F_1 = EA\left(U'_x + \frac{1}{R}U_z\right) + \frac{1}{R}E\hat{I}_2\left(U''_z + \frac{1}{R^2}U_z\right) + \frac{1}{R}E\hat{I}_{2\phi}\left(\theta'' + \frac{1}{R}U''_y\right) + \frac{1}{R}E\hat{I}_{23}\left(U''_y - \frac{1}{R}\theta\right),$$

$$F_2 = -E\hat{I}_3\left(U_y''' - \frac{1}{R}\theta'\right) - \frac{1}{R}E\hat{I}_\phi\left(\theta''' + \frac{1}{R}U_y'''\right) + \frac{1}{R}GJ\left(\theta' + \frac{1}{R}U_y'\right) - \frac{1}{R}E\hat{I}_{2\phi}\left(U_z''' + \frac{1}{R^2}U_z'\right)$$

$$- E\hat{I}_{3\phi}\left\{\frac{1}{R}\left(U_y''' - \frac{1}{R}\theta'\right) + \left(\theta''' + \frac{1}{R}U_y'''\right)\right\} - E\hat{I}_{23}\left(U_z''' + \frac{1}{R^2}U_z'\right) - \rho\omega^2\left(\tilde{I}_3 + \frac{1}{R}\tilde{I}_{3\phi}\right)U_y'$$

$$- \rho\omega^2\left(\frac{1}{R}\tilde{I}_\phi + \tilde{I}_{3\phi}\right)\left(\theta' + \frac{1}{R}U_y'\right) - \rho\omega^2\left(\frac{1}{R}\tilde{I}_{2\phi} + \frac{1}{R}I_{223} + I_{23}\right)\left(U_z' - \frac{1}{R}U_x\right)$$

$$+ \rho\omega^2\frac{1}{R}\left(\frac{1}{R}I_{2\phi} + I_{23}\right)U_x + \left(1 + \frac{\beta}{R^2}\right){}^0F_1U_y' + \frac{\beta}{R}{}^0F_1\theta',$$

$$F_3 = -E\hat{I}_2\left(U_z''' + \frac{1}{R^2}U_z'\right) - E\hat{I}_{2\phi}\left(\theta''' + \frac{1}{R}U_y'''\right) - E\hat{I}_{23}\left(U_y''' - \frac{1}{R}\theta'\right) - \rho\omega^2\tilde{I}_2\left(U_z' - \frac{1}{R}U_x\right)$$

$$+ \rho\omega^2\frac{1}{R}I_2U_x - \rho\omega^2\tilde{I}_{2\phi}\left(\theta' + \frac{1}{R}U_y'\right) - \rho\omega^2\left(\frac{1}{R}I_{223} + I_{23}\right)U_y' + {}^0F_1\left(U_z' - \frac{U_x}{R}\right),$$

$$M_1 = -E\hat{I}_\phi\left(\theta''' + \frac{1}{R}U_y'''\right) + GJ\left(\theta' + \frac{1}{R}U_y'\right) - E\hat{I}_{2\phi}\left(U_z''' + \frac{1}{R^2}U_z'\right) - E\hat{I}_{3\phi}\left(U_y''' - \frac{1}{R}\theta'\right)$$

$$- \rho\omega^2\tilde{I}_\phi\left(\theta' + \frac{1}{R}U_y'\right) - \rho\omega^2\tilde{I}_{3\phi}U_y' - \rho\omega^2\tilde{I}_{2\phi}\left(U_z' - \frac{1}{R}U_x\right)$$

$$+ \rho\omega^2\frac{1}{R}I_{2\phi}U_x + {}^0F_1\beta\left(\theta' + \frac{U_y'}{R}\right),$$

$$M_2 = E\hat{I}_2\left(U_z'' + \frac{1}{R^2}U_z\right) + EI_{2\phi}\left(\theta'' + \frac{1}{R}U_y''\right) + E\hat{I}_{23}\left(U_y'' - \frac{1}{R}\theta\right),$$

$$M_3 = E\hat{I}_3\left(U_y'' - \frac{1}{R}\theta\right) + E\hat{I}_{3\phi}\left(\theta'' + \frac{1}{R}U_y''\right) + E\hat{I}_{23}\left(U_z'' + \frac{1}{R^2}U_z\right),$$

$$M_\phi = E\hat{I}_\phi\left(\theta'' + \frac{1}{R}U_y''\right) + EI_{2\phi}\left(U_z'' + \frac{1}{R^2}U_z\right) + E\hat{I}_{3\phi}\left(U_y'' - \frac{1}{R}\theta\right). \tag{B.3}$$

Appendix C

C.1. The components of matrix **A**

$$\mathbf{A}=\begin{bmatrix}
k_1 & & & & & & & & & & & & \\
& k_2 & & & & & & & & & & & \\
& & k_1 & & & & & & & & & & \\
& & & k_1 & & & & & & & & & \\
& & & & k_1 & & & & & & & & \\
& & & & & k_3 & & & k_4 & & & k_5 & \\
& & & & & & k_1 & & & & & & \\
& & & & & & & k_1 & & & & & \\
& & & & & & & & k_1 & & & & \\
& & & & & k_4 & & & k_6 & & & k_7 & \\
& & & & & & & & & k_1 & & & \\
& & & & & & & & & & k_1 & & \\
& & & & & & & & & & & k_1 & \\
& & & & & k_5 & & & k_7 & & & k_8 &
\end{bmatrix} \tag{C.1}$$

$$k_1=1.0,\quad k_2=-EA,\quad k_3=E\hat{I}_3+\frac{1}{R^2}E\hat{I}_\phi+\frac{2}{R}E\hat{I}_{3\phi},\quad k_4=\frac{1}{R}E\hat{I}_{2\phi}+E\hat{I}_{23},$$

$$k_5=\frac{1}{R}E\hat{I}_\phi+E\hat{I}_{3\phi},\quad k_6=E\hat{I}_2,\quad k_7=E\hat{I}_{2\phi},\quad k_8=E\hat{I}_\phi.$$

C.2. The components of matrix **B**

$$\mathbf{B}=\begin{bmatrix}
& b_1 & & & & & & & & & & & \\
b_2 & & & b_3 & & & & b_4 & & & & b_5 & \\
& & & b_1 & & & & & & & & & \\
& & & & b_1 & & & & & & & & \\
& & & & & b_1 & & & & & & & \\
& b_6 & b_7 & & b_8 & & & & b_9 & & b_{10} & & b_{11} \\
& & & & & & & b_1 & & & & & \\
& & & & & & & & b_1 & & & & \\
& & & & & & & & & b_1 & & & \\
& -b_4 & & & -b_g & & b_{12} & & b_{13} & & b_{14} & & b_{15} \\
& & & & & & & & & & & b_1 & \\
& & & & & & & & & & & & b_1 \\
& & & & & & & & & & & & & b_1 \\
& -b_5 & b_{10} & & b_{11} & & b_{14} & & b_{15} & & b_{16} & & b_{17} &
\end{bmatrix} \tag{C.2}$$

$$b_1 = 1.0, \quad b_2 = \rho\omega^2\left(A + \frac{2I_2}{R^2} + \frac{\tilde{I}_2}{R^2}\right) - \frac{1}{R^2}{}^0F_1,$$

$$b_3 = -\rho\omega^2\frac{1}{R}\left\{\frac{1}{R}(\tilde{I}_{2\phi} + I_{2\phi}) + \left(\frac{I_{223}}{R} + 2I_{23}\right)\right\},$$

$$b_4 = \frac{EA}{R} - \rho\omega^2\frac{1}{R}\left(\tilde{I}_2 + I_2\right) + \frac{1}{R}{}^0F_1, \quad b_5 = -\rho\omega^2\frac{1}{R}(\tilde{I}_{2\phi} + I_{2\phi}),$$

$$b_6 = \rho\omega^2\frac{1}{R}\left(\frac{1}{R}\tilde{I}_{2\phi} + \frac{1}{R}I_{2\phi} + \frac{1}{R}I_{223} + 2I_{23}\right), \quad b_7 = \rho\omega^2 A,$$

$$b_8 = \frac{1}{R^2}GJ - \rho\omega^2\left(\tilde{I}_3 + \frac{1}{R^2}\tilde{I}_\phi + \frac{2}{R}\tilde{I}_{3\phi}\right) + {}^0F_1\left(1 + \frac{\beta}{R^2}\right),$$

$$b_9 = -\left\{\frac{1}{R^3}E\hat{I}_{2\phi} + \frac{1}{R^2}E\hat{I}_{23} + \rho\omega^2\left(\frac{1}{R}\tilde{I}_{2\phi} + \frac{1}{R}I_{223} + I_{23}\right)\right\}, \quad b_{10} = -\frac{1}{R}\rho\omega^2 I_2,$$

$$b_{11} = \frac{1}{R}GJ + \frac{1}{R}E\hat{I}_3 + \frac{1}{R^2}E\hat{I}_{3\phi} - \rho\omega^2\left(\frac{1}{R}\tilde{I}_\phi + \tilde{I}_{3\phi}\right) + \frac{\beta}{R}{}^0F_1,$$

$$b_{12} = -\left(\frac{1}{R^2}EA + \frac{1}{R^4}E\hat{I}_2 - \rho\omega^2 A\right), \quad b_{13} = -\left(\frac{2}{R^2}E\hat{I}_2 + \rho\omega^2\tilde{I}_2 - {}^0F_1\right),$$

$$b_{14} = -\left(\frac{1}{R^3}E\hat{I}_{23} + \frac{1}{R}\rho\omega^2 I_{23}\right), \quad b_{15} = -\left(\frac{1}{R^2}E\hat{I}_{2\phi} - \frac{1}{R}E\hat{I}_{23} + \rho\omega^2\tilde{I}_{2\phi}\right),$$

$$b_{16} = -\left(\frac{1}{R^2}E\hat{I}_3 - \rho\omega^2\tilde{I}_0 - \frac{\beta}{R}{}^0F_1\right), \quad b_{17} = GJ + \frac{2}{R}E\hat{I}_{3\phi} - \rho\omega^2\tilde{I}_\phi + \beta^0F_1.$$

Appendix D

D.1. The components of matrix S

$$\mathbf{S}=\begin{bmatrix} s_1 & s_2 & s_3 & s_4 & s_5 & s_6 & \\ s_7 & s_8 & s_9 & s_{10} & s_{11} & s_{12} & s_{13} \\ s_{14} & s_{15} & s_{16} & s_{17} & s_{18} & s_{19} & s_{20} \\ s_{21} & s_{22} & s_{23} & s_{24} & s_{20} & s_{25} & s_{26} \\ & s_{27} & s_{28} & s_{18} & s_{29} & -s_6 & \\ & s_{30} & -s_5 & s_{31} & s_{32} & s_{33} & \\ & s_{13} & s_{34} & s_{20} & s_{35} & s_{26} & \end{bmatrix} \tag{D.1}$$

$$s_1=EA,\quad s_2=\frac{1}{R}\left(E\hat{I}_{23}+\frac{1}{R}E\hat{I}_{2\phi}\right),\quad s_3=\frac{1}{R}\left(EA+\frac{1}{R^2}E\hat{I}_2\right),\quad s_4=\frac{1}{R}E\hat{I}_2,$$

$$s_5=-\frac{1}{R^2}E\hat{I}_{23},\quad s_6=\frac{1}{R}E\hat{I}_{2\phi},\quad s_7=\rho\omega^2\frac{1}{R}\left(\frac{1}{R}\tilde{I}_{2\phi}+\frac{1}{R}I_{2\phi}+\frac{1}{R}I_{223}+2I_{23}\right),$$

$$s_8=\frac{1}{R^2}GJ-\rho\omega^2\left(\tilde{I}_3+\frac{1}{R^2}\tilde{I}_\phi+\frac{2}{R}\tilde{I}_{3\phi}\right)+{}^0F_1\left(1+\frac{\beta}{R^2}\right),\quad s_9=-\left(E\hat{I}_3+\frac{1}{R^2}E\hat{I}_\phi+\frac{2}{R}E\hat{I}_{3\phi}\right),$$

$$s_{10}=-\left\{\frac{1}{R^3}E\hat{I}_{2\phi}+\frac{1}{R^2}E\hat{I}_{23}+\rho\omega^2\left(\frac{1}{R}\tilde{I}_{2\phi}+\frac{1}{R}I_{223}+I_{23}\right)\right\},\quad s_{11}=-\frac{1}{R}E\hat{I}_{2\phi}-E\hat{I}_{23},$$

$$s_{12}=\frac{1}{R}GJ+\frac{1}{R}E\hat{I}_3+\frac{1}{R^2}E\hat{I}_{3\phi}-\rho\omega^2\left(\frac{1}{R}\tilde{I}_\phi+\tilde{I}_{3\phi}\right)+\frac{\beta}{R}{}^0F_1,\quad s_{13}=-\frac{1}{R}E\hat{I}_\phi-E\hat{I}_{3\phi},$$

$$s_{14}=\frac{1}{R}\left\{\rho\omega^2\left(\tilde{I}_2+I_2\right)-{}^0F_1\right\},\quad s_{15}=-\rho\omega^2\left(\frac{1}{R}\tilde{I}_{2\phi}+\frac{1}{R}I_{223}+I_{23}\right),\quad s_{16}=-E\hat{I}_{23}-\frac{1}{R}E\hat{I}_{2\phi},$$

$$s_{17}=-\left(\frac{1}{R^2}E\hat{I}_2+\rho\omega^2\tilde{I}_2-{}^0F_1\right),\quad s_{18}=-E\hat{I}_2,\quad s_{19}=\frac{1}{R}E\hat{I}_{23}-\rho\omega^2\tilde{I}_{2\phi},\quad s_{20}=-E\hat{I}_{2\phi},$$

$$s_{21}=\rho\omega^2\frac{1}{R}(\tilde{I}_{2\phi}+I_{2\phi}),\quad s_{22}=\frac{1}{R}GJ-\rho\omega^2\left(\tilde{I}_{3\phi}+\frac{1}{R}\tilde{I}_\phi\right)+\frac{\beta}{R}{}^0F_1,\quad s_{23}=-E\hat{I}_{3\phi}-\frac{1}{R}E\hat{I}_\phi,$$

$$s_{24} = -\frac{1}{R^2}E\hat{I}_{2\phi} - \rho\omega^2\tilde{I}_{2\phi}, \quad s_{25} = GJ + \frac{1}{R}E\hat{I}_{3\phi} - \rho\omega^2\tilde{I}_{\phi} + \beta^0 F_1, \quad s_{26} = -E\hat{I}_{\phi},$$

$$s_{27} = -E\hat{I}_{23} - \frac{1}{R}E\hat{I}_{2\phi}, \quad s_{28} = -\frac{1}{R^2}E\hat{I}_2, \quad s_{29} = \frac{1}{R}E\hat{I}_{23}, \quad s_{30} = E\hat{I}_3 + \frac{1}{R}E\hat{I}_{3\phi},$$

$$s_{31} = E\hat{I}_{23}, \quad s_{32} = -\frac{1}{R}E\hat{I}_3, \quad s_{33} = E\hat{I}_{3\phi}, \quad s_{34} = -\frac{1}{R^2}E\hat{I}_{2\phi}, \quad s_{35} = -E\hat{I}_{\phi}.$$

References

[1] K.Y. Nieh, C.S. Huang, Y.P. Tseng, An analytical solution for in-plane vibration and stability of loaded elliptic arches, *Computers and Structures* 81 (2003) 1311–1327.

[2] M. Eisenberger, E. Efraim, In-plane vibrations of shear deformable curved beams, *International Journal for Numerical Methods in Engineering* 52 (2001) 1221–1234.

[3] W.P. Howson, A.K. Jemah, Exact dynamic stiffness method for planar natural frequencies of curved Timoshenko beams, *Proceedings of the Institution of Mechanical Engineers* 213 (1999) 687–696.

[4] C.S. Huang, Y.P. Tseng, A.W. Leissa, K.Y. Nieh, An exact solution for in-plane vibrations of an arch having variable curvature and cross section, *International Journal of Mechanical Sciences* 40 (1998) 1159–1173.

[5] Y.P. Tseng, C.S. Huang, C.J. Lin, Dynamic stiffness analysis for in-plane vibrations of arches with variable curvature, *Journal of Sound and Vibration* 207 (1997) 15–31.

[6] A.K. Gupta, W.P. Howson, Exact natural frequencies of plane structures composed of slender elastic curved members, *Journal of Sound and Vibration* 175 (1994) 145–157.

[7] M.S. Issa, T.M. Wang, B.T. Hsiao, Extensional vibrations of continuous circular curved beams with rotary inertia and shear deformation, I: free vibration, *Journal of Sound and Vibration* 114 (1987) 297–308.

[8] T.M. Wang, M.P. Guilbert, Effects of rotary inertia and shear on natural frequencies of continuous circular curved beams, *International Journal of Solids and Structures* 17 (1981) 281–289.

[9] Z. Friedman, J.B. Kosmatka, An accurate two-node finite element for shear deformable curved beams, *International Journal for Numerical Methods in Engineering* 41 (1998) 473–498.

[10] P. Raveendranath, Gajbir Singh, B. Pradhan, Free vibration of arches using a curved beam element based on a coupled polynomial displacement field, *Computers and Structures* 78 (2000) 583–590.

[11] T. Tarnopolskaya, F.R. De Hoog, N.H. Fletcher, Low-frequency mode transition in the free in-plane vibration of curved beams, *Journal of Sound and Vibration* 228 (1999) 69–90.

[12] T. Tarnopolskaya, F.R. De Hoog, N.H. Fletcher, S. Thwaites, Asymptotic analysis of the free in-plane vibrations of beam with arbitrarily varying curvature and cross-section, *Journal of Sound and Vibration* 196 (1996) 659–680.

[13] S.J. Oh, B.K. Lee, I.W. Lee, Natural frequencies of non-circular arches with rotatory inertia and shear deformation, *Journal of Sound and Vibration* 219 (1999) 23–33.

[14] A. Krishnan, Y.J. Suresh, A simple cubic linear element for static and free vibration analysis of curved beams, *Computers and Structures* 68 (1998) 473–489.

[15] P. Chidamparam, A.W. Leissa, Influence of centerline extensibility on the in-plane free vibrations of loaded circular arches, *Journal of Sound and Vibration* 183 (1995) 779–795.

[16] J.P. Charpie, C.B. Burroughs, An analytic model for the free in-plane vibration of beams of variable curvature and depth, *Journal of the Acoustical Society of America* 94 (1993) 866–879.

[17] J.F.M. Scott, J. Woodhouse, Vibration of an elastic strip with varying curvature, *Philosophical Transactions of the Royal Society of London, Physical Sciences and Engineering* 339 (1992) 587–625.

[18] B.K. Lee, J.F. Wilson, Free vibrations of arches with variable curvature, *Journal of Sound and Vibration* 136 (1989) 75–89.

[19] K. Suzuki, S. Takahashi, In-plane vibration of curved bars with varying cross-section, *Bulletin of the Japan Society of Mechanical Engineers* 25 (1982) 1100–1107.

[20] T. Irie, G. Yamada, I. Takahashi, In-plane vibration of a free-clamped slender arc of varying cross-section, *Bulletin of the Japan Society of Mechanical Engineers* 23 (1980) 567–573.

[21] T.M. Wang, Lowest natural frequency of clamped parabolic arcs, *Journal of Structural Division* 98 (1972) 407–411.
[22] A.S. Veletsos, W.J. Austin, C.A. Lopes, Shyr-jen Wung, Free in-plane vibration of circular arches, *Journal of Engineering Mechanics Division* 98 (1972) 311–329.
[23] M. Petyt, C.C. Fleischer, Free vibration of a curved beam, *Journal of Sound and Vibration* 18 (1971) 17–30.
[24] W.H. Wittrick, F.W. Williams, A general algorithm for computing natural frequencies of elastic structures, *Quarterly Journal of Mechanics and Applied Mathematics* 24 (1971) 263–284.
[25] E.T. Whittaker, G.N. Watson, *A Course of Modern Analysis*, 4th Edition, Cambridge University Press, Cambridge, 1965.
[26] S.Y. Lee, J.C. Chao, Exact solutions for out-of-plane vibration of curved nonuniform beams, *Journal of Applied Mechanics* 68 (2001) 186–191.
[27] C.S. Huang, Y.P. Tseng, S.H. Chang, C.L. Hung, Out-of-plane dynamic analysis of beams with arbitrarily varying curvature and cross-section by dynamic stiffness matrix method, *International Journal of Solids and Structures* 37 (2000) 495–513.
[28] C.S. Huang, Y.P. Tseng, S.H. Chang, Out-of-plane dynamic responses of non-circular curved beams by numerical Laplace transform, *Journal of Sound and Vibration* 215 (1998) 407–424.
[29] W.P. Howson, A.K. Jemah, Exact out-of-plane natural frequencies of curved Timoshenko beams, *Journal of Engineering Mechanics* 125 (1999) 19–25.
[30] W.P. Howson, A.K. Jemah, J.Q. Zhou, Exact natural frequencies for out-of-plane motion of plane structures composed of curved beam members, *Computers and Structures* 55 (1995) 989–995.
[31] K. Kang, C.W. Bert, A.G. Striz, Vibration analysis of horizontally curved beams with warping using DQM, *Journal of Structural Engineering* 215 (1996) 657–662.
[32] V.H. Cortinez, M.T. Piovan, R.E. Rossi, Out of plane vibrations of thin walled curved beams considering shear flexibility, *Structural Engineering and Mechanics* 8 (1999) 257–272.
[33] M.T. Piovan, V.H. Cortinez, R.E. Rossi, Out-of-plane vibrations of shear deformable continuous horizontally curved thin-walled beams, *Journal of Sound and Vibration* 237 (2000) 101–118.
[34] J.M. Snyder, J.F. Wilson, Free vibrations of continuous horizontally curved beams, *Journal of Sound and Vibration* 157 (1992) 345–355.
[35] T.M. Wang, W.F. Brannen, Natural frequencies for out-of-plane vibrations of curved beams on elastic foundations, *Journal of Sound and Vibration* 84 (1982) 241–246.
[36] T.M. Wang, R.H. Nettleton, B. Keita, Natural frequencies for out-of-plane vibrations of continuous curved beams, *Journal of Sound and Vibration* 68 (1980) 427–436.
[37] V. Yildrim, A computer program for the free vibration analysis of elastic arcs, *Computers and Structures* 78 (1997) 475–485.
[38] K. Kang, C.W. Bert, A.G. Striz, Vibration and buckling analysis of circular arches using DQM, *Computers and Structures* 60 (1996) 49–57.
[39] K. Kang, C.W. Bert, A.G. Striz, Vibration analysis of shear deformable circular arches by the differential quadrature method, *Journal of Sound and Vibration* 181 (1995) 353–360.
[40] M. Kawakami, T. Sakiyama, H. Matsuda, C. Morita, In-plane and out-of-plane free vibrations of curved beams with variable sections, *Journal of Sound and Vibration* 187 (1995) 381–401.
[41] M.Y. Kim, N.I. Kim, B.C. Min, Analytical and numerical study on spatial free vibration of non-symmetric thin-walled curved beams, *Journal of Sound and Vibration* 258 (2002) 595–618.
[42] M.Y. Kim, N.I. Kim, H.T. Yun, Exact dynamic and static stiffness matrices of shear deformable thin-walled beam-colums, *Journal of Sound and Vibration* 267 (2003) 29–55.
[43] ABAQUS 1992 User's Manual Vol. I and Vol. II. Ver. 5.2, Hibbit, Karlsson.
[44] Microsoft IMSL Library 1995, Microsoft Corporation.